(1990); D. S. Dessau *et al.*, *ibid.* **71**, 2781 (1993); P. Aebi *et al.*, *ibid.* **72**, 2757 (1994).
3. B. O. Wells *et al.*, *Phys. Rev. B* **46**, 11830 (1992); Z.-X. Shen *et al.*, *Phys. Rev. Lett.* **70**, 1553 (1993); H. Ding *et al.*, *Phys. Rev. B* **54**, R9678 (1996).
4. A. G. Loeser *et al.*, *Science* **273**, 325 (1996).
5. H. Ding *et al.*, *Nature* **382**, 51 (1996).
6. D. Pines and P. Nozieres, *The Theory of Quantum Liquids* (Benjamin, New York, 1969).
7. G. Grimvall, *The Electron-Phonon Interaction in Metals* (North-Holland, New York, 1981).
8. S. Chakravarty, B. I. Halperin, D. R. Nelson, *Phys. Rev. B* **39**, 2344 (1989); S. Sachdev and J. Ye, *Phys. Rev. Lett.* **69**, 2411 (1992); A. Sokol and D. Pines, *ibid.* **71**, 2813 (1993); V. J. Emery and S. A. Kivelson, *ibid.*, p. 3701; C. Castellani, C. Di Castro, M. Grilli, *ibid.* **75**, 4650 (1995); C. M. Varma, *Phys. Rev. B* **55**, 14554 (1997).
9. M. Gurvitch and A. T. Fiory, *Phys. Rev. Lett.* **59**, 1337 (1987).
10. A. V. Puchkov, D. N. Basov, T. Timusk, *J. Phys. Condens. Mater.* **8**, 10049 (1996).
11. The experimental studies reported here were carried out on a Scienta hemispherical analyzer. The instrument has an angular resolution of ±0.1° or better and, in the present studies, an energy resolution of ~10 meV. The total spectral response may be measured as a function of angle and energy simultaneously. Photons were provided either by a resonance lamp or by a normal incidence monochromator based at the National Synchrotron Light Source. In the photon energy range used, 15 to 21.2 eV, the angular resolution of the instrument results in a momentum resolution on the order of 0.005 Å^{-1}. Samples of optimally doped (T_c = 91 K) $Bi_2Sr_2CaCu_2O_{8+\delta}$ produced by the floating zone method [G. D. Gu, K. Takamuku, N. Koshizuka, S. Tanaka, *J. Crystallogr. Growth* **130**, 325 (1990)] were mounted on a liquid He cryostat and cleaved in situ in the ultra-high vacuum chamber with base pressure 2×10^{-9} Pa. During the recording of each spectrum, the temperature was measured with a silicon sensor mounted near the sample.
12. J. E. Inglesfield and E. W. Plummer in *Angle-Resolved Photoemission*, S. D. Kevan, Ed. (Elsevier, Amsterdam, 1992).
13. H. Krakauer and W. E. Pickett, *Phys. Rev. Lett.* **60**, 1665 (1988).
14. N. W. Ashcroft and N. D. Mermin, *Solid State Physics* (Saunders, Philadelphia, PA, 1976), chap. 13.
15. P. B. Allen, in *Quantum Theory of Real Materials*, J. R. Chelikowsky and S. G. Louie, Eds. (Kluwer, Boston, 1996), pp. 219–250.
16. A. V. Fedorov *et al.*, *Phys. Rev. Lett.* **82**, 2179 (1999).
17. T. Valla, A. V. Fedorov, P. D. Johnson, S. L. Hulbert, *ibid.*, **83**, 2085 (1999).
18. C. Olson *et al.*, *Phys. Rev. B* **42**, 381 (1990).
19. C. M. Varma, P. B. Littlewood, S. Schmitt-Rink, E. Abrahams, A. E. Ruckenstein, *Phys. Rev. Lett.* **63**, 1936 (1989).
20. P. W. Anderson, in *Frontiers and Borderlines in Many-Particle Physics* (North-Holland, Amsterdam, 1987).
21. G. Aeppli *et al.*, *Science* **278**, 21 (1997).

22. We thank V. J. Emery, V. N. Muthukumar, R. J. Goodimg, and S. A. Kivelson for useful discussions. Supported in part by the Department of Energy under contract number DE-AC02-98CH10886 and in part by the New Energy and Industrial Technology Development Organization.

28 April 1999; accepted 18 August 1999

Extrusion Polymerization: Catalyzed Synthesis of Crystalline Linear Polyethylene Nanofibers Within a Mesoporous Silica

Keisuke Kageyama, Jun-ichi Tamazawa, Takuzo Aida*

Crystalline nanofibers of linear polyethylene with an ultrahigh molecular weight (6,200,000) and a diameter of 30 to 50 nanometers were formed by the polymerization of ethylene with mesoporous silica fiber–supported titanocene, with methylalumoxane as a cocatalyst. Small-angle x-ray scattering analysis indicated that the polyethylene fibers consist predominantly of extended-chain crystals. This observation indicates a potential utility of the honeycomb-like porous framework as an extruder for nanofabrication of polymeric materials.

Recent developments in polymerization catalysis have enabled the precise control of the primary properties of polymers such as molecular weight, co-monomer sequence, and stereo sequence (*1*). However, for polymers to be used as commodity materials, molecular orientation (crystal structure) (*2*) or morphology (*3, 4*), or both, must also be controlled. Postprocessing steps, such as extrusion or spinning, are usually required to fabricate polymeric materials that perform more elaborate functions. Some crystalline polymers with controlled morphology are already produced in nature. For example, in the biosynthesis of highly crystalline cellulose fibers by the bacterium *Acetobacter xylinum*, cellulose synthase in a cellular membrane forms fine elementary fibrils of cellulose. They are then assembled into macrofibrils and fibers by extrusion through nanopores arranged in the cellular membrane (*5*). A regular arrangement of multiple catalytic sites on mesostructured porous materials could mimic this natural system and produce crystalline polymers with a fibrous morphology (Fig. 1).

We report the production of crystalline polyethylene fibers with a diameter of 30 to 50 nm by the polymerization of ethylene with titanocene (Cp_2Ti, where Cp is the cyclopentadienyl ligand) supported by a fibrous mesoporous silica in conjunction with methylalumoxane (MAO) as a cocatalyst. A mesoporous silica has a honeycomb-like framework with a uniform, controllable pore diameter from 15 to 100 Å (*6*). It is made up of a hexagonal arrangement of the linear channels. Recently, a new class of mesoporous materials called mesoporous silica fiber (MSF) has been developed, consisting of uniformly sized mesopores (27 Å) arranged in a parallel direction to the fiber axis (*7*). This material can be easily prepared by a sol-gel process at a water-oil interface. We used this material as a solid support of titanocene for the polymerization of ethylene (*8, 9*).

The MSF-supported titanocene (Cp_2Ti-MSF) was prepared according to a modified method of Thomas and co-workers (*10*). The powder x-ray diffraction (XRD) pattern of Cp_2Ti-MSF showed peaks characteristic of a hexagonal symmetry with a *d* spacing of 3.8 nm (wall thickness + pore diameter). Similar to the case for MSF (*7*), transmission electron microscopy (TEM) of finely ground Cp_2Ti-MSF showed a clear image of regularly arranged mesoscopic pores with a diameter of 2 to 3 nm.

The polymerization of ethylene with Cp_2Ti-MSF in the presence of MAO gave a cocoon-like solid mass consisting of fibrous polyethylene (PE). For example, a toluene

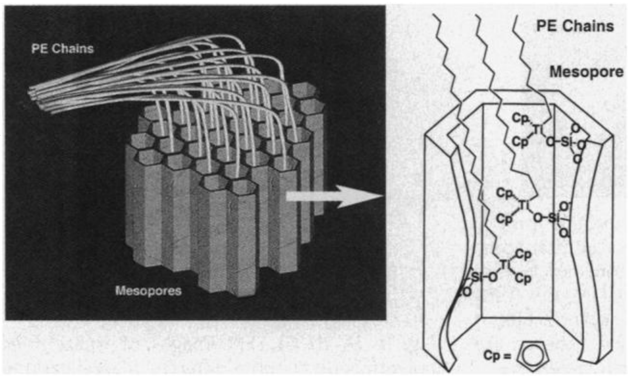

Fig. 1. Conceptual scheme for the growth of crystalline fibers of polyethylene by mesoporous silica–assisted extrusion polymerization.

Department of Chemistry and Biotechnology, Graduate School of Engineering, University of Tokyo, 7-3-1 Hongo, Bunkyo-ku, Tokyo 113-8656, Japan.

*To whom correspondence should be addressed. E-mail: aida@macro.t.u-tokyo.ac.jp

(20 ml) solution of MAO (Al/Ti = 1000) was added under N_2 to a stainless steel autoclave (100 ml) containing dried Cp_2Ti-MSF (50 mg; 3×10^{-6} mol Ti) and a stirring bar in a glass cylinder (diameter = 2.5 cm), and the mixture was stirred for 1 hour at 20°C. The resulting suspension was pressurized by the introduction of ethylene and stirred magnetically under a constant pressure (10 atm) at 20°C. After 4 hours, the autoclave was opened, and the resulting cocoon-like polymeric mass, which absorbed most of the solvent (Fig. 2A), was picked out with tweezers (Fig. 2B) and dipped in a large volume of benzene. After stirring for 48 hours, the polymeric mass was freeze-dried to give 1.8 g of colorless PE. Here, the production rate of PE was estimated to be 15 kg mol^{-1} $hour^{-1}$ bar^{-1}. Quite unexpectedly, the PE thus obtained had an ultrahigh viscometric molecular weight (M_V = 6,200,000) and a higher density (1.01 g cm^{-3}) than that of a PE obtained with a homogeneous system, Cp_2TiCl_2-MAO, under similar conditions (0.97 g cm^{-3}) (*11*). The ^{13}C nuclear magnetic resonance (NMR) spectrum of the PE in 1,2,4-trichlorobenzene-C_6D_6 at 130°C showed a single CH_2 signal at δ 30.1 ppm (*12*), which indicates a linear sequence of the repeating ethylene units without any branch structures.

Scanning electron microscope (SEM) images of the freeze-dried PE reveal bundles of PE fibers (Fig. 3, A and B). When the view was further magnified (field emission SEM), ultrathin discrete fibers with a smooth surface, 30 to 50 nm in diameter, were observed (Fig. 3C). Polarization microscopy of the PE fibers showed a clear birefringence in the fraying edge region, which suggests that the fibers are crystalline. The XRD pattern (Fig. 4A) was typical of crystalline PEs having [110] and [200] diffraction peaks at 21.6° and 23.8°, respectively (*13*), whereas an amorphous halo, which should be observable around 19.6°, was negligibly small. The XRD pattern also showed several other diffraction peaks at 15.3°, 17.4°, 23.0°, 26.7°, 27.4°, and 27.7° that have not been observed for ordinary crystalline PEs. Small-angle x-ray scattering (SAXS) of the crystalline PE fibers (Fig. 4B) showed only a diffuse scattering without any diffraction peaks due to folded-chain crystals (*14*), in contrast with the pattern of a commercial, high-density crystalline PE (Fig. 4C). Thus, the PE fibers consist predominantly of extended-chain crystals. Thermal analysis of the PE fibers by differential scanning calorimetry (DSC; Fig. 5) under unconstrained conditions showed a main endotherm at 140°C with a broad peak centered at a much higher temperature (159°C), where the heat of fusion (ΔH) was evaluated to be 350 J g^{-1}. The PE prepared with the homogeneous Cp_2TiCl_2-MAO system showed a single endotherm at a lower temperature (130°C) with a much smaller ΔH of 207 J g^{-1}. Taking into account the result of SAXS, the broad endotherm centered at 159°C (Fig. 5) is attributable to the phase transition of the extended-chain crystals from an orthorhombic phase to a hexagonal phase and the melting of the hexagonal phase (*15*). In the second stage of heating, such a high-temperature endotherm was no longer observed, whereas only a single peak (T_m) was observed at a lower temperature (130°C). Furthermore, the several distinctive XRD peaks observed in Fig. 4A also disappeared when the PE fibers were melted.

From these observations, it is evident that each PE fiber consists of extended-chain crystals, but the fibers are not regularly oriented, leading to the formation of a porous cocoon-like assembly with a large surface area. Thus, the extraordinary peaks in the XRD pattern (Fig. 4A) may be attributed to specific diffractions of the PE crystals in the surface domain of the fiber, which must be different from those of the orthorhombic crystalline phase in the inner domain.

For the formation of the crystalline PE fibers with the MSF-supported titanocene (Cp_2Ti-MSF), we postulate an "extrusion polymerization" mechanism (Fig. 1) similar to the biosynthesis of crystalline cellulose. Polymer chains, formed at the activated titanocene sites within the individual mesopores, are extruded into the solvent phase and assembled to form extended-chain crystalline fibers. As the pore

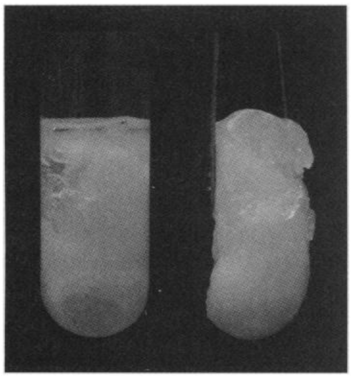

Fig. 2. Polymerization of ethylene (10 atm) in toluene at 20°C with MSF-supported titanocene (50 mg, 3×10^{-6} mol Ti) in conjunction with MAO (Al/Ti = 1000) [Cp_2Ti-MSF-MAO]. (Left) Polymerization mixture in a glass cylinder after 4 hours. (Right) Solvent-absorbing, cocoon-like polymeric product picked out with tweezers.

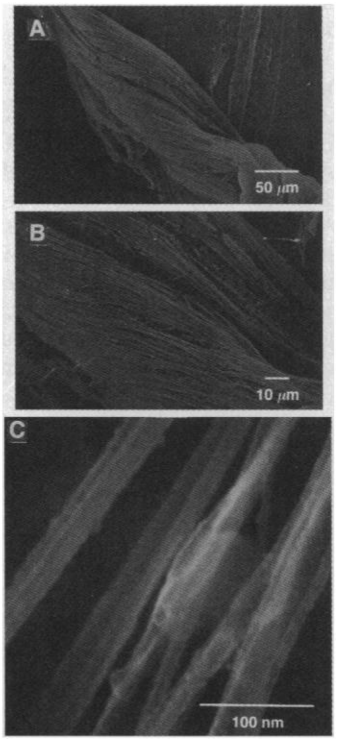

Fig. 3. (**A** to **C**) SEM images of freeze-dried polyethylene at three different magnifications.

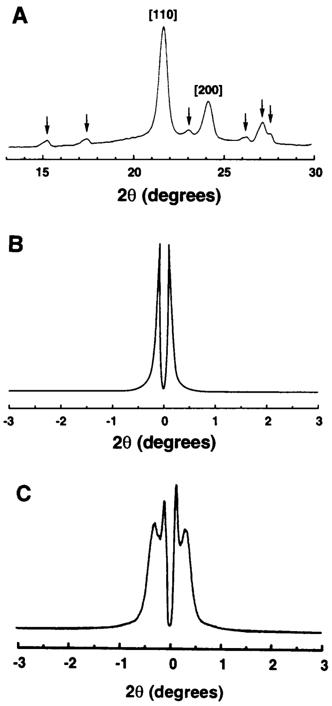

Fig. 4. (**A**) XRD pattern (indexed peaks: assigned to orthorhombic phase) and (**B**) SAXS pattern of polyethylene fibers freeze-dried from benzene. (**C**) A typical SAXS pattern of a commercial, high-density crystalline polyethylene, for comparison.

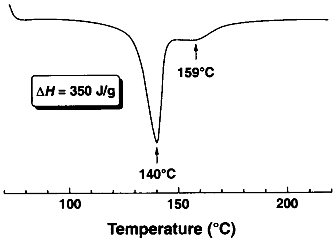

Fig. 5. DSC melting curve of polyethylene fibers freeze-dried from benzene.

diameter of the MSF (27 Å) is much smaller than the lamellar length of ordinary PE crystals (~100 Å) (*16*), the PE chains are likely prevented from folding within the mesopores. To lend support to the extrusion polymerization mechanism, we evaporated a reaction mixture of Cp_2Ti-MSF with MAO in toluene to dryness and exposed the residue to ethylene. The SEM images of the polymerization mixture (Fig. 6) indicated the formation of PE only on the circular cross sections of the silica fibers where the pore exits are opened.

When a nonfibrous mesoporous silica such as MCM-41 (*6*) was used in place of MSF as the solid support of titanocene, a crystalline PE containing a fibrous fraction was obtained (*17*). However, it showed ordinary XRD and DSC patterns (a single endotherm at 142°C; $\Delta H = 222$ J g^{-1}). On the other hand, use of an amorphous silica–supported titanocene-MAO system (*17*) for the polymerization resulted in neither fibrous texture nor extraordinary XRD and DSC profiles of the product (a single endotherm at 140°C; $\Delta H = 167$ J g^{-1}).

It has been reported that a fibrous PE with a diameter of 0.2 to 0.5 μm, containing a fraction of extended-chain crystals, can be obtained by crystallization of PE from a vigorously stirred xylene solution (*18*). In contrast, our approach is based on an essentially different conception, namely template-assisted extrusion polymerization. Regularly arranged nanoscopic pores on a honeycomb-like solid surface enable in situ formation of much thinner (30 to 50 nm) PE fibers of extended-chain crystals. The present method, using MSF as a nano-extruder, may be widely applicable to the production of fabricated crystalline polymers. Moreover, the use of mesoporous materials of different architectures as templates for polymerization is expected to provide common polymers with some new bulk properties.

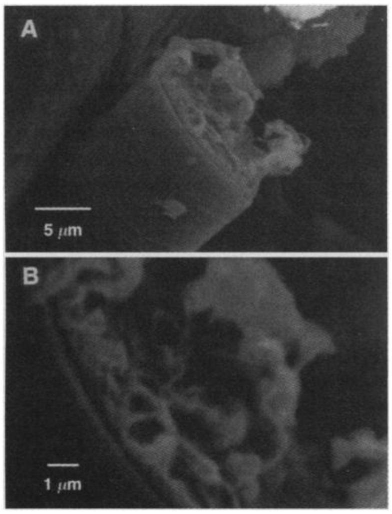

Fig. 6. (**A** and **B**) SEM images of a piece of Cp_2Ti-MSF, treated with a toluene solution of MAO (Al/Ti = 1000), dried under reduced pressure, and then exposed to ethylene (10 atm), at two different magnifications.

References and Notes

1. O. W. Webster, *Science* **251**, 887 (1991); Y. Okamoto and T. Nakano, *Chem. Rev.* **94**, 349 (1994); S. Kobayashi, Ed., *Catalysis in Precision Polymerization* (Wiley, New York, 1997).
2. P. Smith and P. J. Lemstra, *J. Mater. Sci.* **15**, 505 (1980); J. C. M. Torfs and A. J. Pennings, *J. Appl. Polym. Sci.* **26**, 303 (1981); J. H. Lee, R. M. Brown Jr., S. Kuga, S. Shoda, S. Kobayashi, *Proc. Natl. Acad. Sci. U.S.A.* **91**, 7425 (1994).
3. E. Evans, H. Bowman, A. Leung, D. Needham, D. Tirrel, *Science* **273**, 933 (1996); S. B. Roscoe, J. M. Fréchet, J. F. Walzer, A. J. Dias, *ibid.* **280**, 271 (1998); K. Akagi *et al.*, *ibid.* **282**, 1683 (1998).
4. D. A. Tomalia, *Adv. Mater.* **6**, 529 (1994); D.-L. Jiang and T. Aida, *Nature* **388**, 454 (1997); M. Fisher and F. Vögtle, *Angew. Chem. Int. Ed.* **38**, 884 (1999).
5. T. P. Nevell, Ed., *Cellulose Chemistry and Its Applications* (Halsted, New York, 1985), chap. 2.
6. J. S. Beck *et al.*, *J. Am. Chem. Soc.* **114**, 10834 (1992); A. Corma, *Chem. Rev.* **97**, 2373 (1997).
7. G. D. Stucky *et al.*, *Adv. Mater.* **9**, 974 (1997).
8. For examples of polymerization with mesoporous materials, see C.-G. Wu and T. Bein, *Science* **266**, 1013 (1994); S. M. Ng, S. Ogino, T. Aida, K. A. Koyano, T. Tatsumi, *Macromol. Rapid Commun.* **18**, 991 (1997); K. Kageyama, S. Ogino, T. Aida, T. Tatsumi, *Macromolecules* **31**, 4069 (1998).
9. For examples of olefin polymerization with mesoporous materials, see Y.-S. Ko, T.-K. Han, J.-W. Park, S.-I. Woo, *Macromol. Rapid Commun.* **17**, 749 (1996); J. Tudor and D. O'Hare, *Chem. Commun.* **1997**, 603 (1997); L. K. M. van Looveren *et al.*, *Angew. Chem. Int. Ed.* **37**, 517 (1998).
10. MSF (0.3 g) was treated with a dichloromethane solution of titanocene dichloride (Cp_2TiCl_2) at 20°C in the presence of triethylamine as a proton scavenger. After stirring for 18 hours, an insoluble material was isolated by filtration and washed repeatedly with dichloromethane. The amount of Cp_2Ti mounted on the MSF surface was 6×10^{-5} mol Ti g^{-1} (Si/Ti = 280), as determined by inductively coupled plasma mass spectrometry (ICP-MS). See T. Maschmeyer, F. Rey, G. Sankar, J. M. Thomas, *Nature* **378**, 159 (1995).
11. Measured using a flotation method with methanol/dioxane at 30°C.
12. G. B. Galland, R. F. de Souza, R. S. Mauler, F. F. Nunes, *Macromolecules* **32**, 1620 (1999).
13. S. Krimm and A. V. Tobolsky, *J. Polym. Sci.* **7**, 57 (1951).
14. B. G. Rånby, F. F. Morehead, N. M. Walter, *ibid.* **44**, 349 (1960); L. Mandelkern, A. S. Posner, A. F. Diorio, D. E. Roberts, *J. Appl. Phys.* **32**, 509 (1961).
15. A. J. Pennings and A. Zwijnenburg, *J. Polym. Sci. Polym. Phys. Ed.* **17**, 1011 (1979).
16. W. D. Niegisch and P. R. Swan, *J. Appl. Phys.* **31**, 1906 (1960).
17. Prepared by a method similar to that for the preparation of Cp_2Ti-MSF. The amounts of Cp_2Ti mounted on MCM-41 and amorphous silica were both 5×10^{-5} mol Ti g^{-1}. Polymerization conditions: supported catalyst, 50 mg (2.5×10^{6} mol) Ti; cocatalyst, MAO (Al/Ti = 500); ethylene pressure, 10 atm; 20°C, 13.5 hours. PE yields: 1.8 g Cp_2Ti–MCM-41–MAO, 1.0 g Cp_2Ti–amorphous silica–MAO.
18. A. J. Pennings, C. J. H. Schouteten, A. M. Kiel, *J. Polym. Sci. C* **38**, 167 (1972).

19. Partly supported by a grant-in-aid from the Ministry of Education, Science, Sports, and Culture, Japan, and by a grant from the New Energy and Industrial Technology Development Organization under the Ministry of International Trade and Industry, Japan. We thank S. Tanji, K. Ebara, and O. Mitsui for obtaining the viscometric molecular weight of PE and the SEM pictures of Cp_2Ti-MSF, T. Sugawara for obtaining FE-SEM pictures of polyethylene fibers, and A. Takahara for discussion. K.K. thanks the Japan Society for the Promotion of Science for a Young Scientist Fellowship.

11 June 1999; accepted 30 July 1999

Primordial Noble Gases from Earth's Mantle: Identification of a Primitive Volatile Component

M. W. Caffee,[1] G. B. Hudson,[1] C. Velsko,[1] G. R. Huss,[2] E. C. Alexander Jr.,[3] A. R. Chivas[4]

Carbon dioxide well gases in Colorado, New Mexico, and South Australia show excesses of $^{124-128}$Xe correlated with ^{129}I-derived ^{129}Xe and ^{20}Ne/^{22}Ne ratios that are higher than the atmospheric ^{20}Ne/^{22}Ne ratio. The xenon isotopic data indicate the presence of a solarlike component deep within Earth. The presence of this component in crustal and upper mantle reservoirs may be explained by a steady-state transport of noble gases from the lower mantle, which still retains much of its juvenile volatile inventory. These measurements also indicate that the mantle source of these noble gases in the carbon dioxide well gases cannot be the source of Earth's present atmosphere. The variations observed in ^{129}Xe/^{130}Xe between solar wind xenon, Earth's atmosphere, and mantle samples may be generated by variations of iodine/xenon in terrestrial reservoirs, as opposed to rapid early degassing.

The detailed nature of Earth's precursor material, the structure and volatile inventory of Earth's mantle, and the relation of the atmosphere to more primitive reservoirs within Earth are elusive problems that continue to be addressed with elemental and isotopic abundance studies (*1, 2*). The scarcity of the noble gases in naturally occurring materials, their chemical inertness, and the presence of distinct identifiable isotopic and elemental compositions make noble gases ideal tracers for many of these investigations (*3–5*). Recognizing the difference between the noble gas signature in Earth's present atmosphere and

LINKED CITATIONS

You have printed the following article:

Extrusion Polymerization: Catalyzed Synthesis of Crystalline Linear Polyethylene Nanofibers Within a Mesoporous Silica

Keisuke Kageyama; Jun-ichi Tamazawa; Takuzo Aida

Science, New Series, Vol. 285, No. 5436. (Sep. 24, 1999), pp. 2113-2115.

Stable URL:

http://links.jstor.org/sici?sici=0036-8075%2819990924%293%3A285%3A5436%3C2113%3AEPCSOC%3E2.0.CO%3B2-Y

This article references the following linked citations:

References and Notes

[1] **Living Polymerization Methods**

Owen W. Webster

Science, New Series, Vol. 251, No. 4996. (Feb. 22, 1991), pp. 887-893.

Stable URL:

http://links.jstor.org/sici?sici=0036-8075%2819910222%293%3A251%3A4996%3C887%3ALPM%3E2.0.CO%3B2-J

[2] **Assembly of Synthetic Cellulose I**

Jong H. Lee; R. Malcolm Brown, Jr.; Shigenori Kuga; Shin-Ichiro Shoda; Shiro Kobayashi

Proceedings of the National Academy of Sciences of the United States of America, Vol. 91, No. 16. (Aug. 2, 1994), pp. 7425-7429.

Stable URL:

http://links.jstor.org/sici?sici=0027-8424%2819940802%2991%3A16%3C7425%3AAOSCI%3E2.0.CO%3B2-%23

[3] **Biomembrane Templates for Nanoscale Conduits and Networks**

Evan Evans; Howard Bowman; Andrew Leung; David Needham; David Tirrell

Science, New Series, Vol. 273, No. 5277. (Aug. 16, 1996), pp. 933-935.

Stable URL:

http://links.jstor.org/sici?sici=0036-8075%2819960816%293%3A273%3A5277%3C933%3ABTFNCA%3E2.0.CO%3B2-J

[3] **Polyolefin Spheres from Metallocenes Supported on Noninteracting Polystyrene**

Stephen B. Roscoe; Jean M. J. Fréchet; John F. Walzer; Anthony J. Dias

Science, New Series, Vol. 280, No. 5361. (Apr. 10, 1998), pp. 270-273.

Stable URL:

http://links.jstor.org/sici?sici=0036-8075%2819980410%293%3A280%3A5361%3C270%3APSFMSO%3E2.0.CO%3B2-S

NOTE: *The reference numbering from the original has been maintained in this citation list.*

LINKED CITATIONS

- Page 2 of 2 -

[3] **Helical Polyacetylene Synthesized with a Chiral Nematic Reaction Field**
K. Akagi; G. Piao; S. Kaneko; K. Sakamaki; H. Shirakawa; M. Kyotani
Science, New Series, Vol. 282, No. 5394. (Nov. 27, 1998), pp. 1683-1686.
Stable URL:
http://links.jstor.org/sici?sici=0036-8075%2819981127%293%3A282%3A5394%3C1683%3AHPSWAC%3E2.0.CO%3B2-3

[8] **Conducting Carbon Wires in Ordered, Nanometer-Sized Channels**
Chun-Guey Wu; Thomas Bein
Science, New Series, Vol. 266, No. 5187. (Nov. 11, 1994), pp. 1013-1015.
Stable URL:
http://links.jstor.org/sici?sici=0036-8075%2819941111%293%3A266%3A5187%3C1013%3ACCWION%3E2.0.CO%3B2-4

NOTE: *The reference numbering from the original has been maintained in this citation list.*